JPEDAV (2006) 27:684-690
DOI: 10.1361/154770306X153747
1547-7037/$19.00 ©ASM International

Internal Carburization and Carbide Precipitation in Fe-Ni-Cr Alloy Tubing Retired from Ethylene Pyrolysis Service

A. Chauhan, M. Anwar, K. Montero, H. White, and W. Si

(Submitted March 23, 2006; in revised form May 10, 2006)

The events leading to the failure of an alloy grade HP Nb ethylene pyrolysis heater tubing were examined. X-ray maps indicated that a complex oxide coating, which inhibits carbon (C) diffusion, forms on the process side of the tubing during service. Phase equilibria studies predict that even without process C diffusion, metal carbides will precipitate out of the face centered cubic (FCC_A1) matrix. It was estimated that a 6 mm thick tube operating at 1100 °C would completely carburize in two years if the protective coating is damaged.

Keywords CALPHAD, multicomponent diffusion, x-ray analysis

1. Introduction

Products derived from ethylene continue to displace conventional materials in packaging, building, automotive, and other applications. The demand for ethylene, one of the highest production chemical commodities in the world, is expected to exceed 136 million metric tons by the year 2010.[1] The production of ethylene involves the steam cracking of feedstocks, ranging from ethane to gas oils, inside the coils of a pyrolysis furnace.[2-4] The overall reaction is free radical in nature and is unselective, with a range of hydrocarbons and coke being produced as byproducts. During catalytic coke formation, the feedstock interacts with the tube wall and deposits carbon (C) on the surface.[5-7] Coke formation is particularly damaging to the overall process because it accumulates on the inner walls of the coils and eventually leads to process inefficiencies (localized increases in tube wall temperatures, poor heat transfer, increased pressure drop, reduction of inner tube diameter, and tube plugging) and tube failure.[8,9] The tube failure modes initiated by catalytic coke formation are: thermal shock; stress rupture; melting; thermal fatigue; and carburization-induced mid wall cracking.[10,11]

The production of ethylene is one of the most energy-intensive processes in the chemical industry because furnace tubes must be decoked every 10 to 80 days (depending on feedstock, furnace type, and severity of operation) to preserve tube life.[12,13] Decoking is started with steam after lowering the temperature to about 800 °C and is continued with a steam-air mixture up to about 1100 °C.[14] The combination of in-service operation and decoking cycles have reduced the tube life of outlet coils by four to six years.[15] High-temperature pyrolysis of hydrocarbons has been practiced for over a half century and still ethylene producers worldwide currently consume $600 million per year of iron (Fe)-nickel (Ni)-chromium (Cr) alloy tubular products. The market is typically 80% maintenance or retubing of existing furnaces and 20% new installations.[1]

Researchers have attempted to limit coke formation in ethylene pyrolysis coils (i.e., increase tube life) by adding small amounts of a variety of inhibitors to the feedstock[5,16-20] and by changing or altering the materials of construction.[5,18-25] The challenge has been developing a material with sufficient high-temperature (~1100 °C) creep strength, sufficient ductility at 1100 °C to withstand in-service stresses, and sufficient ductility below 700 °C after service aging to withstand startup and shutdown stresses. Cast and wrought materials have been designed with specific chemistry in the range of 20 to 35 wt.% Cr, 20 to 45% Ni with the balance typically consisting of Fe plus other important alloying elements such as C, niobium (Nb), W, Ti, Al, Zr, and Mo. Jones[26] compared the wrought (low C) and centrifugally cast (high C) tube materials, and found that the centrifugally cast alloys only satisfy the first two design criteria while the wrought materials suffer from creep damage while in service.

This study presents diffusion-, precipitation-, and phase equilibria-related phenomena of alloy grade HP Nb, a centrifugally cast austenitic microalloyed Ni-Cr-Fe alloy [0.45wt.%C-~1.5wt.%manganese (Mn)-~2.2wt.%silicon (Si)-35wt.%Ni-25wt.%Cr-1.2wt.%Nb-balFe] decommissioned from ethylene pyrolysis service.

2. Experimental

HP Nb tubing (250 mm in length × 120 mm in diameter × 6 mm in thickness) removed from an ethylene pyrolysis

This article was presented at the Multicomponent-Multiphase Diffusion Symposium in Honor of Mysore A. Dayananda, which was held during TMS 2006, 135th Annual Meeting and Exhibition, March 12-16, 2006, in San Antonio, TX. The symposium was organized by Yongho Sohn of University of Central Florida, Carelyn E. Campbell of National Institute of Standards and Technology, Richard D. Sisson, Jr. of Worcester Polytechnic Institute, and John E. Morral of Ohio State University.

A. Chauhan, M. Anwar, K. Montero, and **H. White,** Department of Materials Science and Engineering, Stony Brook University, Stony Brook, NY 11794-2275; and **W. Si,** Department of Condensed Matter Physics and Materials Science, Brookhaven National Laboratory, Upton, NY 11973-5000. Contact e-mail: hwhite@notes.cc.sunysb.edu.

plant during a scheduled retubing was supplied by ABB Lummus Global Incorporated (Bloomfield, NJ). A 12 × 12 × 6 mm section of the tubing was removed and mounted in cross section in a vacuum-impregnated epoxy. The sample was prepared using standard metallographic specimen preparation techniques and examined (with energy-dispersive spectroscopy, x-ray mapping, and backscatter electron micrographs) using the LEO 1550 Shottky field emission gun-scanning electron microscope at Stony Brook University. Phase equilibria studies were performed using Thermocalc and the TTNi Database.[27]

3. Results and Discussion

3.1 Diffusion and Precipitation Phenomena

Several researchers have proposed models and have provided explanations for the carburization of pyrolysis tubing.[14,28-38] Goldstein and Moren[28] studied the diffusion of C in the ternary Fe-C-*M* systems (where M = Cr, Si, or Mn) utilizing Fick's second law for a ternary system to describe the diffusion process.

$$\frac{dC_C}{dt} = D_{CC}^{Fe}\frac{\partial^2 C_C}{\partial x^2} + D_{CM}^{Fe}\frac{\partial^2 C_M}{\partial x^2} \quad \text{(Eq 1)}$$

$$\frac{dC_M}{dt} = D_{MM}^{Fe}\frac{\partial^2 C_M}{\partial x^2} + D_{MC}^{Fe}\frac{\partial^2 C_C}{\partial x^2} \quad \text{(Eq 2)}$$

In these equations, C is the concentration of carbon and the metal M (i.e., Cr, Si, or Mn); D_{MM} and D_{CC} measure the effects of the concentration gradient of a given component on its own flux, and D_{MC} and D_{CM} measure cross effects or ternary diffusional interactions. They further stated that D_{MM} is negligible because it diffuses via substitutional mechanisms (its value should be 10^4 to 10^6 time less than D_{CC}, which diffuses via interstitial mechanisms); D_{MC} is small ($=0$); and D_{CM} and D_{CC} can be estimated using an expression proposed by Brown and Kirkaldy.[39] This study did not include stainless steel compositions and did not consider the effect of carbide precipitation on C diffusion. Bongartz et al.[40] and Zhu et al.[41] developed models for carbide precipitation events during the carburization process. These studies: coupled the effects of C diffusion and carbide precipitation; considered as separate entities of C in the matrix and in the carbide; only allowed the C in the matrix to diffuse; and allowed carbide precipitates to serve as obstacles that slow down the carburization process.

In the current study, a complex oxide protective coating, which formed on the HP Nb alloy surface in service prevented the diffusion of C into the material from the process stream. Figure 1 shows a backscattered electron image and x-ray maps of the HP Nb alloy prior to service. The x-ray maps indicate that all elements [C, Cr, Fe, Nb, Ni, Si, and oxygen (O)] are uniformly distributed in the matrix. The Fe-Si-Nb-Cr collage shows traces for Cr carbide that exist in the matrix. The large concentration of C at the surface is due to the sample preparation consumables.

Figure 2 shows backscattered electron images and x-ray maps of the diffusion and carbide precipitation behavior of HP Nb tubing that was decommissioned from ethylene pyrolysis service during a schedule retubing. While in service: Cr oxide forms at the surface; Si oxide forms beneath the Cr oxide surface layer; metal carbides (mostly Cr) precipitate in the bulk; and Fe, Ni, and Nb remain uniformly distributed in the matrix.

3.2 Phase Equilibria Predicted by ThermoCalc[42,43]

Isothermals (900, 1000, 1100, and 1200 °C) of the seven-component C-Mn-Si-Ni-Cr-Nb-Fe system are shown in Fig. 3. Because the inlet and midsection tube metal temperatures are typically between 900 and 1000 °C, the outlet tube metal temperature is typically between 1000 and 1100 °C, and localized regions where coke deposits exist could reach temperatures of ~1200 °C; the selected isotherm for the multicomponent system can be used to predict the internal carburization and carbide precipitation behavior of the tubing. Table 1 summarizes these features.

At 900 and 1000 °C, $M_{23}C_6$ and σ initially exist in the FCC_A1 matrix (Fig. 3 at 0.45% C). As internal carburization proceeds (green dotted line), $M_{23}C_6$ and M_7C_3 will initially coexist (Fig. 3 at for instance 2% C), and eventually $M_{23}C_6$ will convert to M_7C_3 (Fig. 3 at higher C percentages). Bongartz et al.,[40] Zhu et al.,[41] and Christ[44] have proposed the following equations for the formation of $M_{23}C_6$ and M_7C_3, and the transformation of $M_{23}C_6$ to M_7C_3.

$$16Cr + 7Fe + 6C = Cr_{16}Fe_7C_6 \quad \text{(Eq 3)}$$

$$7Cr + 7Fe + 6C = 2Cr_{3.5}Fe_{3.5}C_3 \quad \text{(Eq 4)}$$

$$54C + 7Cr_{16}Fe_7C_6 + 63Fe \rightarrow 32Cr_{3.5}Fe_{3.5}C_3 \quad \text{(Eq 5)}$$

A similar situation exists at higher temperatures, with the only difference being an increase in the amounts of C and Cr that exist in the FCC_A1 matrix (see the tie-line through 3% C on each phase diagram). The maximum amount of C-Cr in the FCC_A1 matrix that can exist prior to graphite precipitation can also be determined from the phase diagrams (see location marked "*" on each of the phase diagrams and Table 1). Using these values and an expression that describes the depth of the internal carbide formation zone,[45] a rough estimate can be made of the time required for through-wall carburization (Eq 6).

$$t = \frac{x^2 * \nu * C_{Cr}}{2 * \varepsilon * D_C * C_C} \quad \text{(Eq 6)}$$

In this equation, ν is a stoichiometric factor, C_{Cr} is the Cr content in the FCC_A1 matrix before graphite starts to precipitate, C_C is the C content in the FCC_A1 matrix before graphite starts to precipitate, x is the tube wall thickness, D_C is the C diffusivity (~10^{-7} cm^2/s from Nishiyama et al.[46]), and ε ranges from 0 to 1. For values of $\varepsilon < 1$, carbide formation slows the diffusion of C into the matrix.[47] Con-

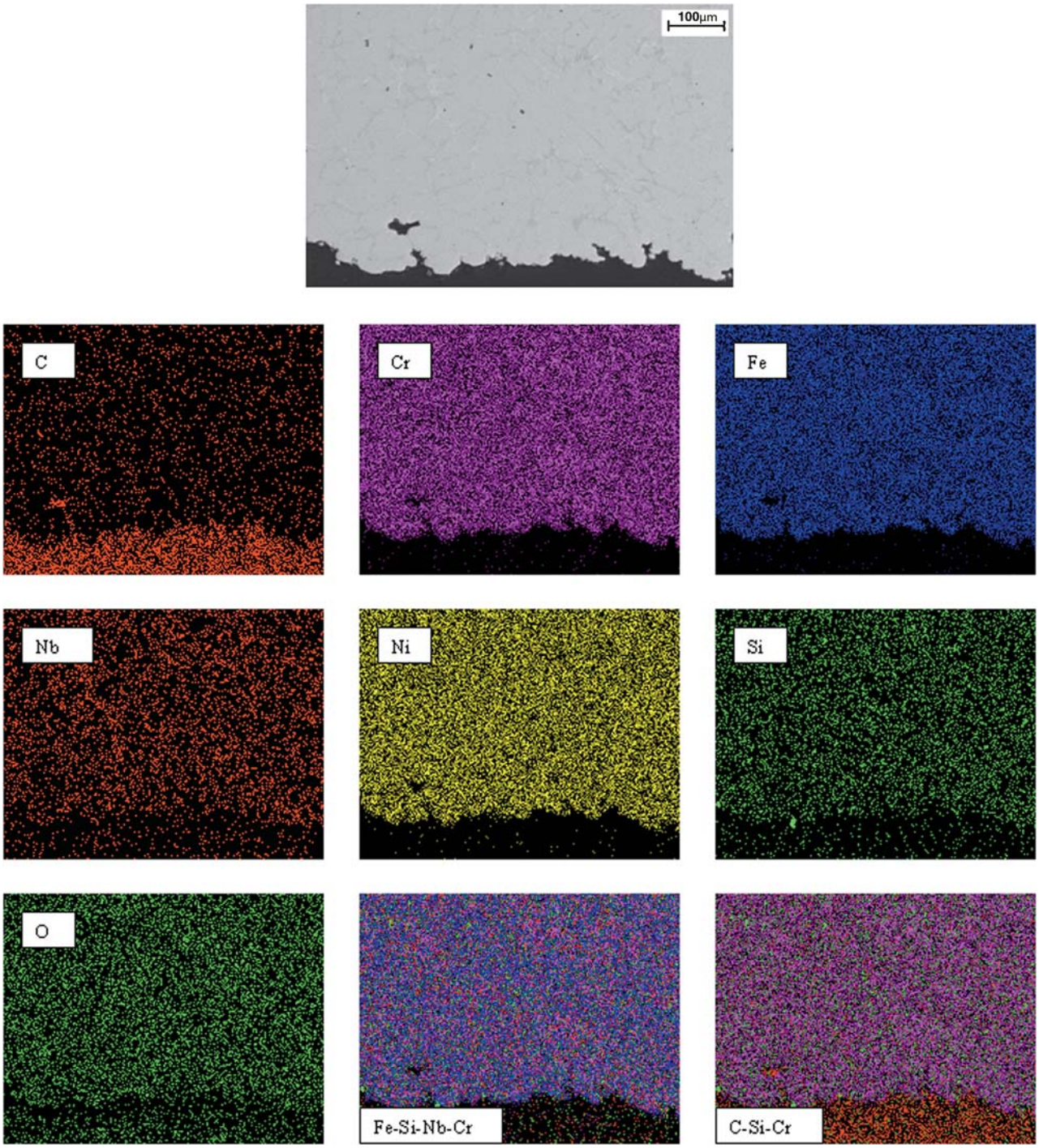

Fig. 1 Backscatter electron image (top) and x-ray maps (C, Cr, Fe, Nb, Ni, Si, O, and collages) of HP Nb tubing prior to service. All elements are uniformly distributed in the matrix. The large content of C at the surface is due to the sample preparation consumables.

sidering that carbides will impede C diffusion ($\varepsilon = 0.5$): $D_C = 10^{-7}$ cm^2/s; $\upsilon = 3$; $x = 6$ mm; and C_C and C_{Cr} values can be obtained from Table 1 (C-Cr content in FCC_A1 before graphite starts to precipitate). The estimated time for complete through-wall carburization of HP Nb tubing that has been exposed to ethylene pyrolysis service at 1100 °C was determined to be approximately two years.

4. Conclusions

An austenitic heat-resistant alloy, HP Nb, which was removed during a scheduled retubing from an ethylene pyrolysis furnace, was examined. X-ray maps indicated that Cr and Si segregate to the surface to form a complex oxide coating, which prevented process C diffusion; beneath the

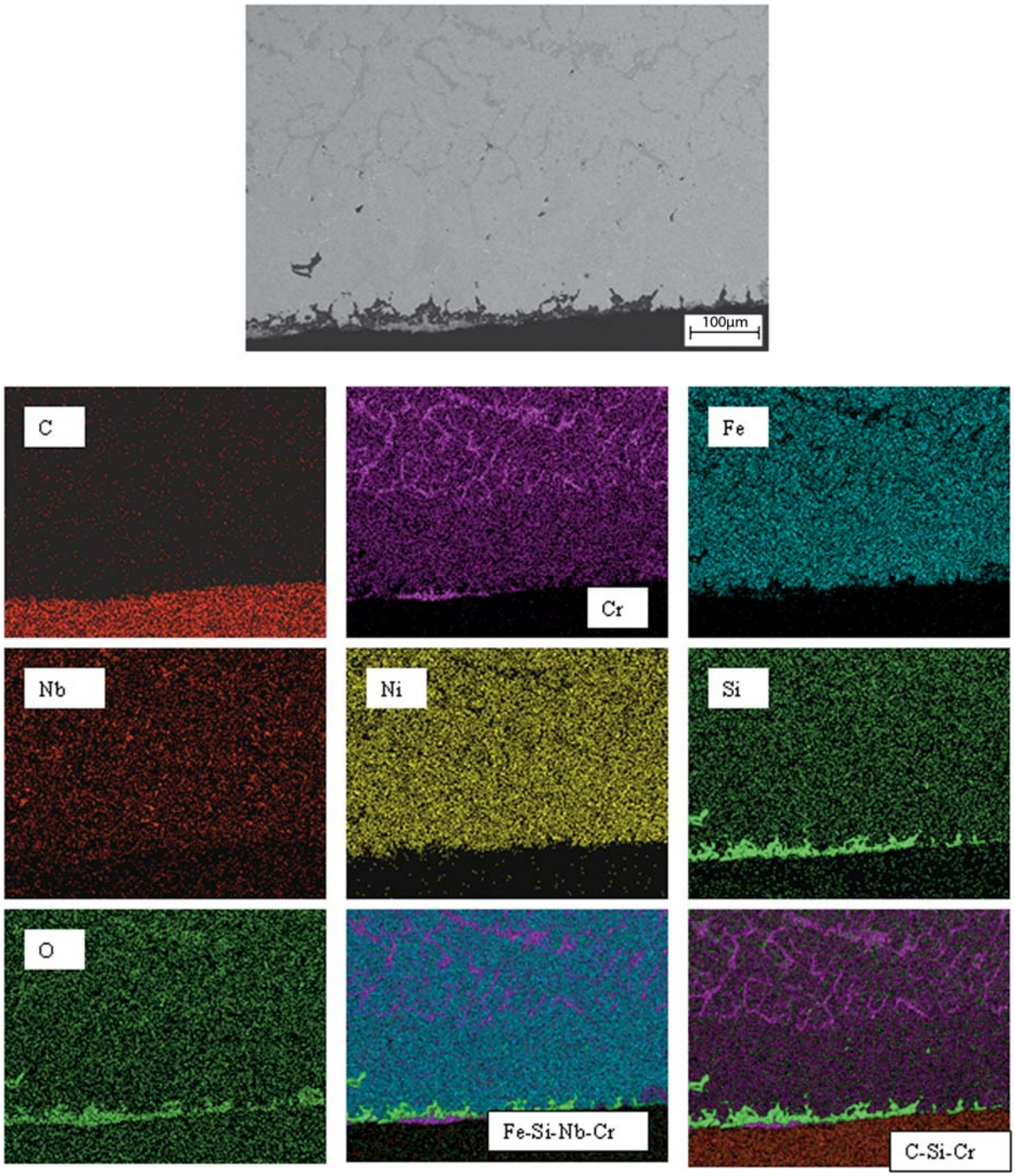

Fig. 2 Backscatter electron image (top) and x-ray maps (C, Cr, Fe, Nb, Ni, Si, O, and collages) of HP Nb tubing removed from ethylene pyrolysis service during a scheduled retubing. The C is from the metallographic mount; Cr segregates to the bulk in the form of carbides and to the surface in the form of oxides; Fe, Nb, and Ni are uniformly distributed in the matrix; and Si and O are found near the surface. Cr oxide and Si oxide protective layers effectively prevented process C diffusion.

protective layer, Cr is depleted from the FCC_A1 matrix; and the bulk metal carbides (mostly Cr) precipitate out of the FCC_A1 matrix.

Phase equilibria predicted by ThermoCalc showed that: even without process C diffusion metal carbides ($M_{23}C_6$) will exist in the FCC_A1 matrix; if the local internal C content increases, $M_{23}C_6$ readily transforms to M_7C_3 type carbides; and if process C diffusion occurs (i.e., oxide layers are damaged as described by Smith et al.[45]), Cr will be depleted from the FCC_A1 matrix and complete carburization of a 6 mm tube wall can occur in approximately two years.

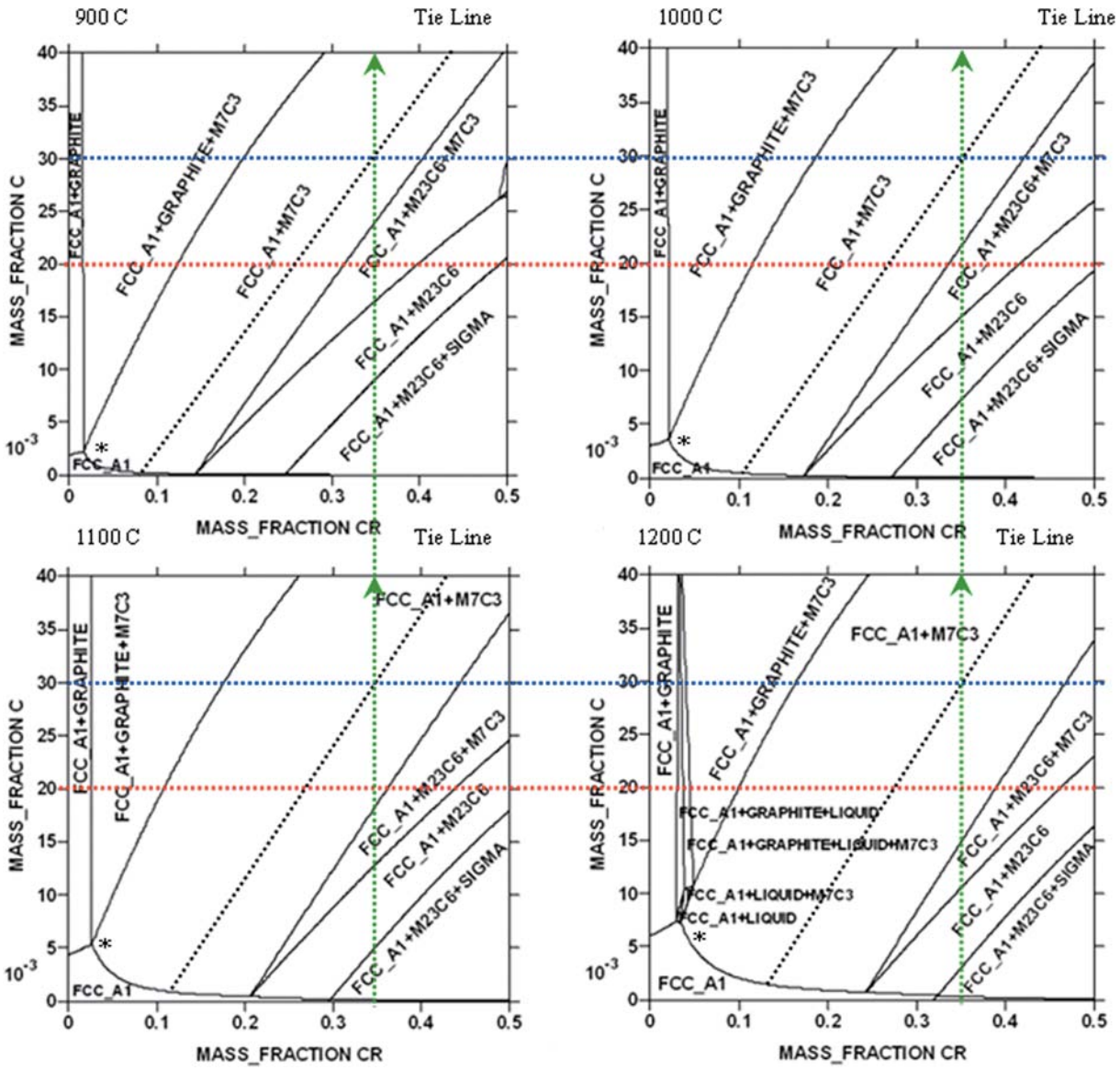

Fig. 3 Phase equilibria predicted by ThermoCalc of HP Nb at 900, 1000, 1100, and 1200 °C. In all cases, as the C content in the material increases (green lines), $M_{23}C_6$ will eventually transform into M_7C_3. *, C and Cr content in which graphite starts to precipitate. At 1200 °C, melting may occur in the C-Cr content where graphite starts to precipitate.

Table 1 HP Nb phase equilibria predicted by ThermoCalc

Phases	900 °C	1000 °C	1100 °C	1200 °C
Initial phase present 0.45 wt.% C	FCC_A1 + $M_{23}C_6$ + σ	FCC_A1 + $M_{23}C_6$ + σ	FCC_A1 + $M_{23}C_6$	FCC_A1 + $M_{23}C_6$
Phases present at local 2 wt.% C	FCC_A1 + $M_{23}C_6$ + M_7C_3	FCC_A1 + $M_{23}C_6$ + M_7C_3	FCC_A1 + M_7C_3	FCC_A1 + M_7C_3
Phases present at local 3 wt.% C	FCC_A1 + M_7C_3	FCC_A1 + M_7C_3	FCC_A1 + M_7C_3	FCC_Al + M_7C_3
C content in FCC_A1 at 3 wt.% C	~0.05%	~0.1%	~0.15%	~0.2%
Cr content in FCC_A1 at 3 wt.% C	~7.5%	~10%	~12%	~13.5%
C content in FCC_A1 before graphite precipitation	~0.2%	~0.35%	~0.51%	~0.7%
Cr content in FCC_A1 before graphite precipitation	~2.5%	~3%	~3.2%	~4%

Acknowledgments

The authors would like to thank Fran Loeb (Brookhaven National Laboratory) for his assistance with sample preparation and Dr. Jim Quinn (Stony Brook University) for his assistance with scanning electron microscope studies. Dr. White would like to thank Dr. Kandasamy Sundaram (ABB Lummus Global) for contributing the samples for this study

and for the 20 years of discussion. This work was supported in part by the National Science Foundation under grant No. 0346947.

References

1. C.A. Sorrell, "Industrial Materials for the Future," report I-XAM-778, U.S. Department of Energy, 2001
2. A.K.K. Lee and A.M. Aitani, Saudi Ethylene Plants Move Toward More Feed Flexibility, *Oil Gas J.,* 1990, **88**(Sept 10), p 60–63
3. K.W. Otto, Olefin Capacity Surge Will Tighten Feedstock Supplies, *Oil Gas J.,* 1989, **3,** p 35-39
4. S. Field, Ethylene Profitability Trends, *Hydrocarbon Process.,* 1990, **69,** p 47-49
5. L.L. Crynes and B.L. Crynes, Coke Formation on Polished and Unpolished Incoloy 800 Coupons during Pyrolysis of Light Hydrocarbons, *Ind. Eng. Chem. Res.,* 1987, **26,** p 2139-2144
6. D.L. Trimm, Fundamental Aspects of the Formation and Gasification of Coke, *Pyrolysis: Theory & Industrial Practice,* L.F. Albright, B.L. Crynes, and W.H. Corcoran, Ed., Academic Press, 1983, Chapter 9, p 203-232
7. L.F. Albright and J.C. Marek, Mechanistic Model for Formation of Coke in Pyrolysis Units Producing Ethylene, *Ind. Eng. Chem. Res.,* 1988, **27,** p 755-759
8. K.M. Sundaram and G.F. Froment, Kinetics of Coke Deposition in the Thermal Cracking of Propane, *Chem. Eng. Sci.,* 1979, **34,** p 635-644
9. K.Y.G. Chan, F. Inal, and S. Senkan, Suppression of Coke Formation in the Steam Cracking of Alkanes: Ethane and Propane, *Ind. Eng. Chem. Res.,* 1998, **37,** p 901-907
10. M.W. Mucek, Laboratory Detection of Degree of Carburization in Ethylene Pyrolysis Furnace Tubing, *Mater. Perform.,* 1983, **9,** p 25-28
11. G.L. Swales, Materials Selection Consideration for Petrochemical Furnace Tubes, *Rev. Int. Hautes Temp. Refract.,* 1976, **13,** p 146-159
12. K.M. Sundaram and G.F. Froment, Kinetics of Coke Deposition in the Thermal Cracking of Propane, *Chem. Eng. Sci.,* 1979, **34,** p 635-644
13. K.M. Sundaram, P.S. Van Damme, and G.F. Froment, Coke Deposition in the Thermal Cracking of Ethane, *AlChE J.,* 1981, **27**(6), p 946-951
14. H.J. Grabke and D. Jakobi, High Temperature Corrosion of Cracking Tubes, *Mater. Corros.,* 2002, **53,** p 494-499
15. S. Ibarra, Materials of Construction in Ethylene Pyrolysis-Heater Service, *Pyrolysis: Theory & Industrial Practice,* L.F. Albright, B.L. Crynes, and W.H. Corcoran, Ed., Academic Press, 1983, p 427–436
16. Z. Renjun, *Fundamentals of Pyrolysis in Petrochemistry and Technology,* CRC Press, Boca Raton, 1993
17. K.G. Burns, D.J. Ciarella, C.T. Rowe, J.L. Sigmon, Chemicals Increase Ethylene Plant Efficiency, *Hydrocarbon Process.,* 1991, **70,** p 83-87
18. D.T. Wickham, J. Engel, and M.E. Karpuk, "Methods for Suppression of Filamentous Coke Formation," U.S. Patent 6,482,311, November 19, 2002
19. Z. Renjun, L. Qiangkun, L. Huicai, and N. Fenghui, Investigation of Coke Deposition during the Pyrolysis of Hydrocarbon, *Ind. Eng. Chem. Res.,* 1987, **26,** p 2528-2532
20. D.L. Trimm, A. Holmen, and O. Lindvag, Coke Formation During Cracking of Hydrocarbons: I. The Effect of Presulphiding on Coke Formation on a Nickel- Chromium-Iron Alloy Under Steam Cracking Conditions, *J. Chem. Technol. Biotechnol.,* 1981, **31,** p 311-316
21. L.F. Albright and J.C. Marek, Coke Formation During Pyrolysis: Roles of Residence Time, Reactor Geometry and Time of Operation, *Ind. Eng. Chem. Res.,* 1988, **27,** p 743-751
22. P.R.S. Jackson, D.L. Trimm, and D.J. Young, The Coking Kinetics of Heat Resistant Austenitic Steels in Hydrogen-Propylene Atmospheres, *J. Mater. Sci.,* 1986, **21,** p 3125-3134
23. D.E. Brown, J.T.K. Clark, J.J. McCarroll, and M.C. Sims, German Patent 2,613,787, October 21, 1976
24. P.R.S. Jackson, D.J. Young, and D.L. Trimm, Coke Deposition on and Removal from Metals and Heat-Resistant Alloys Under Steam-Cracking Conditions, *J. Mater. Sci.,* 1986, **21,** p 4376-4384
25. F. Ropital, A. Sugier, and M. Bisiaux, Etude De La Restauration Des Caracteristiques De Tubes De Four De Vapocraquage En Manaurite 36 XS, *Rev. Inst. Fr. Pet.,* 1989, **44**(1), p 91-100
26. J.J. Jones, *Cast Manifolds, Collectors and Transfer Lines,* APV Paramount Ltd., England, 1988
27. L. Hoglund, *Thermo-Calc: Foundation of Computational Thermodynamics,* Royal Institute of Technology, Stockholm, Sweden, Stockholm, Sweden
28. J.I. Goldstein and A.E. Moran, Diffusion Modeling of the Carburization Process, *Metall. Trans. A,* 1978, **9a,** p 1515-1525
29. A. Schnaas and H.J. Grabke, Changes in Material Properties of Austenitic CrNiFe-Alloys by Carburization, *Werkst. Korros.,* 1978, **29,** p 635-644
30. K. Ledjeff, A. Rahmel, and M. Schorr, Oxidation and Carburization of High Alloyed Materials for Cracking Tubes-Part 1: The Oxidation Behavior in Air, *Werkst. Korros.,* 1979, **30,** p 767-784
31. K. Ledjeff, A. Rahmel, and M. Schorr, Oxidation and Carburization of High Alloyed Materials for Cracking Tubes-Part 2: The Carburization Behavior in Oxygen and Carbon Containing Atmospheres with High Carbon Activity, *Werkst. Korros.,* 1980, **31,** p 83-97
32. H.J. Grabke, K. Ohla, J. Peters, and I. Wolf, Radiotracer Studies of Carbon Permeation through Oxide Scales on Commercial High Temperature Alloys and Model Alloys, *Werkst. Korros.,* 1983, **34,** p 495-500
33. I. Wolf and H.J. Grabke, A Study on the Carbon Solubility and Distribution of Oxides, *Solid State Commun.,* 1985, **54,** p 5-10
34. H.J. Grabke and I. Wolf, Carburization and Oxidation, *Mater. Sci. Eng.,* 1987, **87,** p 23-33
35. I. Wolf, H.J. Grabke, and H.P. Schmidt, Carbon Transport Through Oxide Scales on Fe-Cr Alloys, *Oxid. Met.,* 1988, **29,** p 289-306
36. H.J. Grabke and A. Schnaas, W. Betteridge, et al. Ed., *Review on High Temperature Gaseous Corrosion and Mechanical Performance in Carburizing and Oxidizing Environments,* Alloy 800, North-Holland, Amsterdam, 1978, p 195–211
37. J. Hemptenmacher and H.J. Grabke, Effects of Small Alloying Additions of Niobium or Cerium on the Corrosion and Creep of Incoloy 800 in CO-H_2O-H_2-Atmospheres, *Werkst. Korros.,* 1983, **34,** p 333-340
38. J. Hemptenmacher, G. Sauthoff, and H.J. Grabke, Effects of Carburization of the Creep Behavior of a FeNiCr-High Temperature Alloy, *Werkst. Korros.,* 1984, **35,** p 247-253
39. L.C. Brown and J.S. Kirkaldy, Carbon Diffusion in Dilute Ternary Austenites, *Trans. TMS-AIME,* 1964, **230,** p 223-226
40. K. Bongartz, D.F. Lupton, and H. Schuster, A Model to Predict Carburization Profiles in High Temperature Alloys, *Metall. Trans. A,* 1980, **11,** p 1883-1893

41. M. Zhu, Q. Xu, and J. Zhang, Numerical Simulation of Reaction-Diffusion During Carburization of HK40 Steel, *J. Mater. Sci. Technol.,* 2003, **19**(4), p 327-330
42. N. Saunders and A.P. Miodownik, *CALPHAD: A Comprehensive Guide,* Cambridge, 1998
43. I. Ansara and M.H. Rand, The Industrial Use of Thermodynamical Data, *Thermodynamic Calculations in C-Cr-Fe-Ni System,* T.I. Barry, Ed.. Chemical Society, London, 1980, p 246-257
44. H.-J. Christ, Experimental Characterization and Computer-Based Description of the Carburization Behavior of the Austenitic Stainless Steel AISI 304L, *Mater. Corros.,* 1998, **49,** p 258-265
45. G.M. Smith, D.J. Young, and D.L. Trimm, Carburization Kinetics of Heat Resistant Steels, *Oxid. Met.,* 1982, **18,** p 229-243
46. Y. Nishiyama, N. Otsuka, and T. Nishizawa, Carburization Resistance of Austenitic Alloys in CH_4-CO_2-H_2 Gas Mixtures at Elevated Temperatures, *Corrosion,* 2003, **59,** p 688–700
47. H.J. Grabke, Corrosion of Alloy 600 in a Carburization Furnace, *Mater. Corros.,* 2001, **52,** p 546-551